Physica D 37 (1989) 406–416
North-Holland, Amsterdam

A LIQUID FILM (SOAP FILM) TUNNEL TO STUDY TWO-DIMENSIONAL LAMINAR AND TURBULENT SHEAR FLOWS

Morteza GHARIB and Philip DERANGO
Department of Applied Mechanics and Engineering Sciences, University of California, San Diego, La Jolla, CA 92093, USA

A new experimental approach to study two-dimensional flow phenomena is presented which uses a novel device capable of producing purely two-dimensional flows. In this new technique, a suspended liquid film (a soap film) is set in motion in a long frame using a planar water jet as a pulling mechanism. By producing film velocities up to 250 cm/s, this device can generate a variety of shear flows for quantitative studies via laser Doppler velocimetry. Several examples of shear flows are presented. It is shown that this device can be a valuable tool in establishing a quantitative experimental basis for two-dimensional flows including wakes, jets, mixing layers and grid-generated turbulence.

1. Introduction

The importance of theoretical and experimental studies of two-dimensional flows is long-standing and well known. These studies have significant implications when one deals with the crucial topics of two-dimensional turbulence, transition mechanisms in shear flows, and the fundamentals of two-dimensional vortex dynamics as it relates to oceanic and atmospheric problems.

Theoretical studies of two-dimensional flows have been more prevalent than experimental studies. Numerous theories and models have evolved from these studies which include cascading turbulence models (reviewed by Kraichnan and Montgomery [1]), dynamic meteorology (Lilly [2], Rhines [3]), the structure of viscous wall layers (Jimenez et al. [4]) and vortex dynamics (Aref [5]).

The experimental verification of these hypotheses is seldom decisive, owing in part to the difficulty of isolating the primary two-dimensional flow from evolving three-dimensional instabilities in an experiment. Some characteristics of two-dimensional vortex flows and turbulence were observed in bulk fluids when either rotation (Hopfinger et al. [6]) or a magnetic field (Sommeria and Moreau [7]) was used to create strong anisotropy. The results of these experiments are generally inconclusive due to the problems arising from the complicated nature of the experimental set-ups.

Mysels [8] in his ingenious work on liquid films proposed soap films as a potential candidate to produce and study two-dimensional hydrodynamics. The work of Couder and Basdevant [9] on the dynamics of the vortex wake behind a towed cylinder in a soap film frame proved the feasibility of this potential. However, limitations associated with the short period of observation, non-uniform film thickness and lack of a quantitative technique for flow measurements have limited the wide range use of the towing technique.

Recently, we have invented a continuously running soap film tunnel (Gharib and Derango [10]) which has eliminated the short observation period and non-uniform film thickness problems. This tunnel is essentially a two-dimensional counterpart of conventional wind and water tunnels. The present paper is concerned with application of this novel device to the fundamental problems of two-

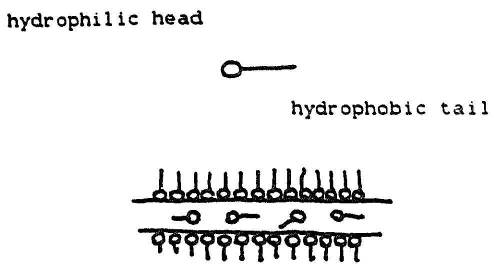

Fig. 1. Molecular structure of a soap molecule and film.

dimensional hydrodynamics. The following sections present the basic operational concept of the soap film tunnel and sample flows generated by it.

1.1. *Some physical properties of soap films*

A soap film is a thin slab of water protected by two monolayers of surfactant. Each surfactant molecule has a polar head facing the water and an aliphatic tail directed toward the air (fig. 1). In a mobile film situation, the two surface layers have a liquid-like behavior and move together with the interstitial liquid (Mysels [8]). The film viscosity consists of the contributions made by the two surfaces – their surface viscosity – and by the intralamellar liquid. The former contribution is the product of the thickness of the liquid and its normal (three-dimensional) viscosity. The resulting viscosity μ_F of the film is given by Trapeznikov [9] as

$$\mu_F = \mu_b + 2\frac{\mu_s}{e},$$

where μ_b is the bulk viscosity of the fluid, μ_s the surface viscosity of the superficial layers, and e the thickness of the film.

The role of pressure is played by surface tension in the film and that of compressibility by Gibbs or Marangoni elasticity. The thickness of the film is an active scalar which responds to the dynamics of the film motion in a manner similar to shallow water flows. In thick films (1 to 10 μm), this small thickness variation results in interference patterns, thus providing an excellent means for flow visualization. Couder et al. [12], in a paper in this issue, present a detailed discussion of the general hydrodynamics of soap films.

2. Soap film tunnel

The device consists of a frame (4 inches wide and 12 inches long), one end of which is positioned in a diluted soap mixture while the other end is subjected to a film-pulling mechanism. The frame is constructed of either copper or glass (fig. 2). The main portion of the frame is a flat section consisting of two parallel rods. This flat section is supported by two legs, one at each end. In our device, the pulling mechanism is provided through the contact action of a two-dimensional water jet. The pulling effect of the high momentum water jet results in a uniform two-dimensional motion of the soap film in the frame. The two-dimensional

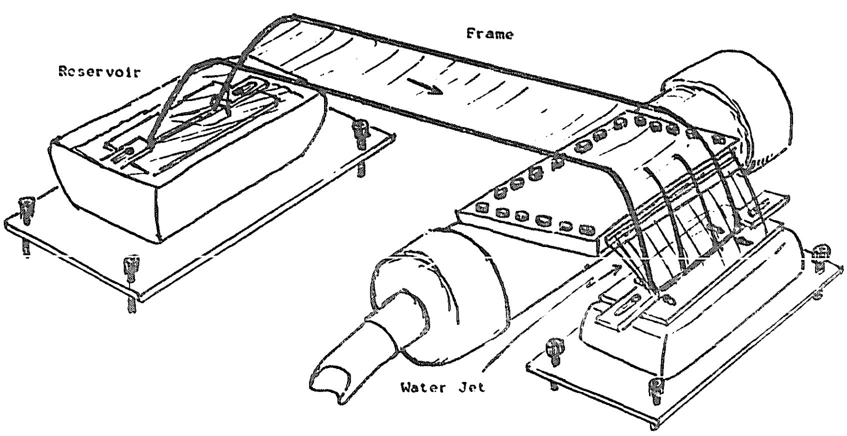

Fig. 2. Schematics of the soap film tunnel.

water jet of higher surface tension is directed at a small angle to the soap film surface. Notice that the leg at the film/water jet interface has fork-like structures. These structures help to stabilize the film/water jet interface.

The size of the frame is limited by the film's tendency to bow at flat sections of the tunnel. The optimum width of the frame to avoid this effect is 4". The streamwise length of the test section can be extended up to 1.5 ft without greatly reducing the life of the film. An average life of the film flow is about 50 min. Several parameters can contribute to the shortening of the film life including dry air, severe ventilation, vibration and unsteadiness or turbulence in the water jet.

Once the two-dimensional flow of the thin film starts in the frame, various objects can be placed in the test section of the frame to study their associated two-dimensional flow fields. By imposing certain geometries on the boundaries of the frame, various shear flows such as jets and two-dimensional mixing layers can be produced.

3. Representative two-dimensional flows

In this section a series of two-dimensional flows are presented to demonstrate the capabilities of the soap film tunnel. With thin films, which have large viscosities, a series of low Reynolds number flows can be produced. One such flow is the flow around a circular cylinder. At low Reynolds numbers (below the onset Reynolds number [$Re \approx 40$] where vortex shedding starts), the flow shows a symmetric stable circular region with two counter-rotating vortices similar to the three-dimensional counterparts (fig. 3). As the Reynolds number increases, this bubble becomes unstable, and for $Re > 40$ it starts to form the celebrated Kármán vortex street (fig. 4).

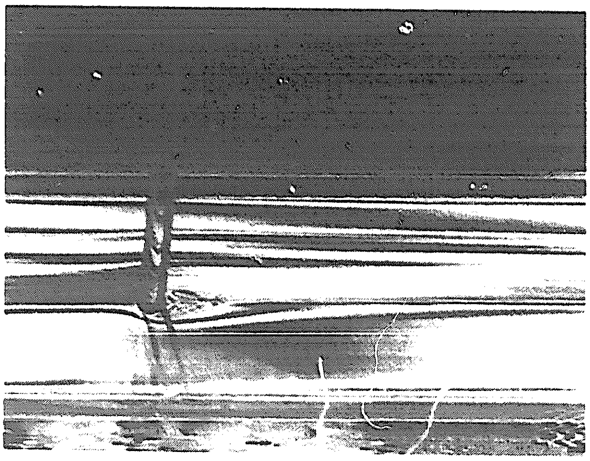

Fig. 3. Low Reynolds number flow around a circular cylinder ($Re = 38$).

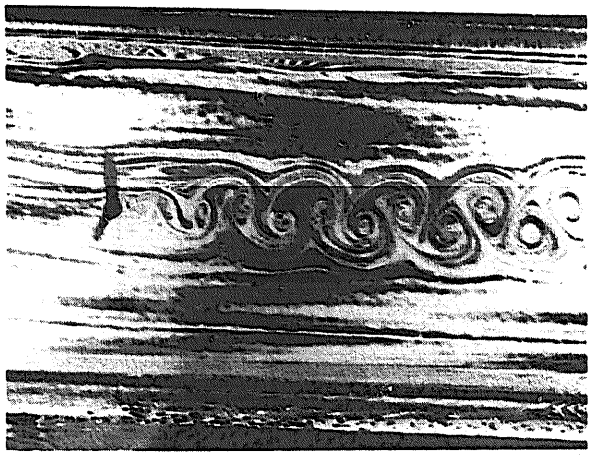

Fig. 4. Kármán vortex wake system behind a circular cylinder ($Re = 110$).

The circulating flow inside a cavity is presented in fig. 5. The next figure shows the flow over a backward facing step and its associated separated mixing layer (fig. 6). An example of grid turbulence generated in the soap film tunnel is presented in fig. 7. Plate I presents evolution and non-linear saturation of two-dimensional instabilities into large coherent vortical structures in a two-dimensional jet. It is important to note that a typical structure of one centimeter in diameter has a depth of only one micron which assures its two-dimensionality. The color flow visualization is due to the interference process [8].

4. Velocity measurement in soap films

Aside from fascinating flow patterns that can be generated in soap films, one needs to develop a

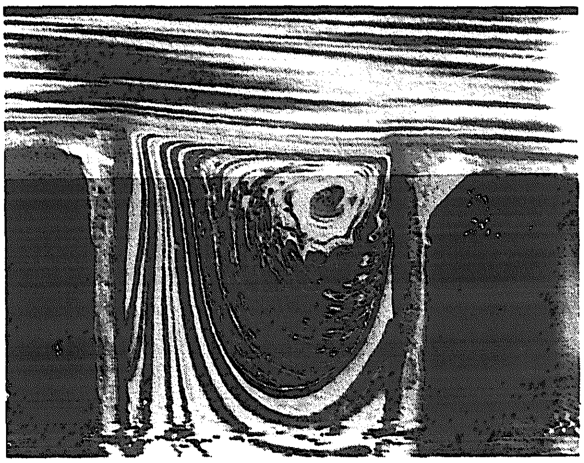

Fig. 5. Cavity flow.

quantitative method to measure the velocity field and its associated characteristics in order to study two-dimensional flows. In this regard we have employed a commercial laser Doppler system to measure the velocity field in our soap film tunnel. A schematic of the laser Doppler system is presented in fig. 8. It should be mentioned that the quality of the Doppler signal that can be obtained in the soap film tunnel surpasses that of the conventional wind or water tunnels. This is due to the fact that the scattering length is confined to the probed section of the film. Therefore, the optical path of the laser beams is essentially noise-free.

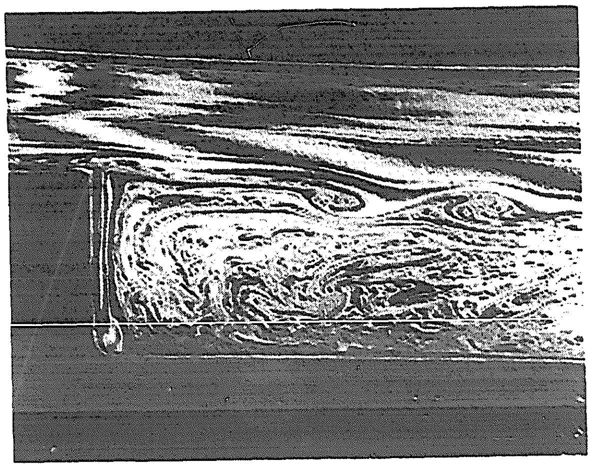

Fig. 6. Flow over a backward-facing step. (Notice the large vortical structures in the separated shear layer.)

Figs. 9(a) and 9(b) present the mean velocity profile measured by laser Doppler across the test section of the soap film tunnel at two streamwise positions. These velocity profiles show good uniformity over a major portion of the measuring section, except for the boundary layers near the wall. Figs. 10(a) and 10(b) show the time series and associated power spectrum for the cylinder wake presented in fig. 4. Figs. 11(a) and 11(b) show mean and fluctuating velocity profiles in the same cylinder wake.

5. Determination of the film viscosity

In order to determine the flow Reynolds number, one needs to estimate the film viscosity. As was mentioned before, the film viscosity consists of two parts: the bulk viscosity and the surface viscosity. Trapeznikov [11] does not suggest any practical method to obtain the surface viscosity. This leaves the evaluation of film viscosity to empirical methods.

One main question is whether the dynamics of the film motion resemble that of its three-dimensional counterparts. For example, the phenomenon of vortex shedding behind a circular cylinder is known to follow the empirical relationship suggested by Roshko [13]. Roshko showed that the Strouhal number and the Reynolds num-

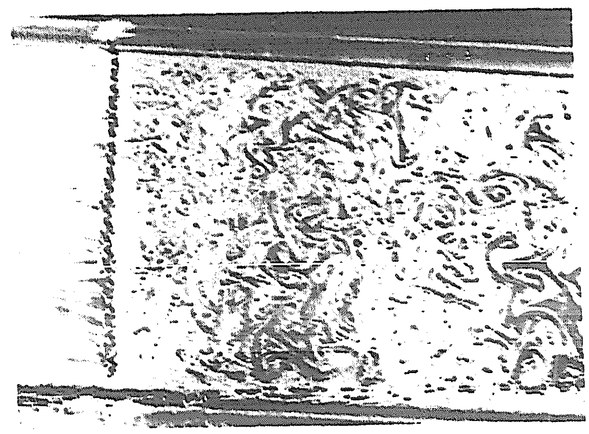

Fig. 7. Two-dimensional grid turbulence.

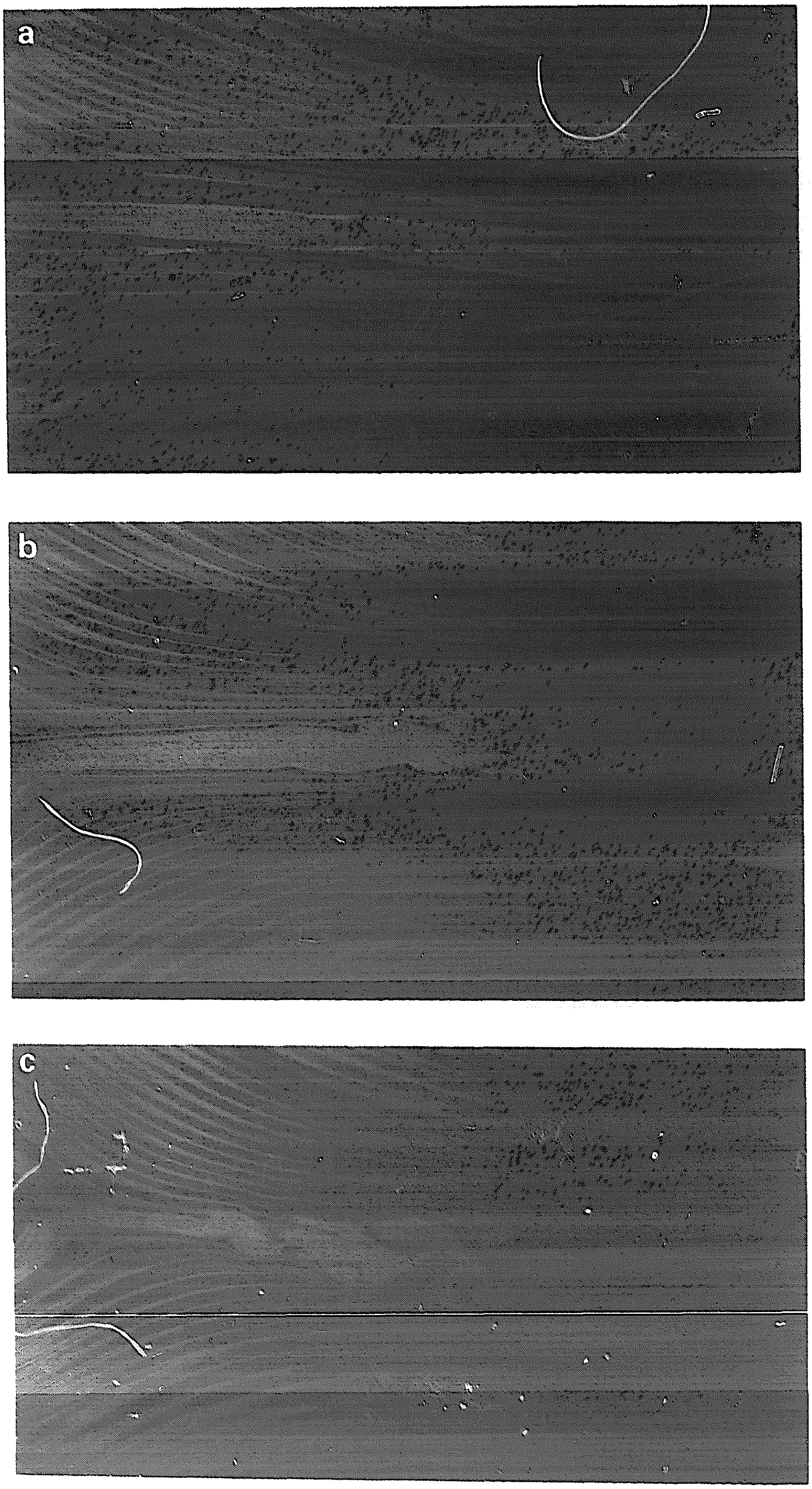
a
b
c

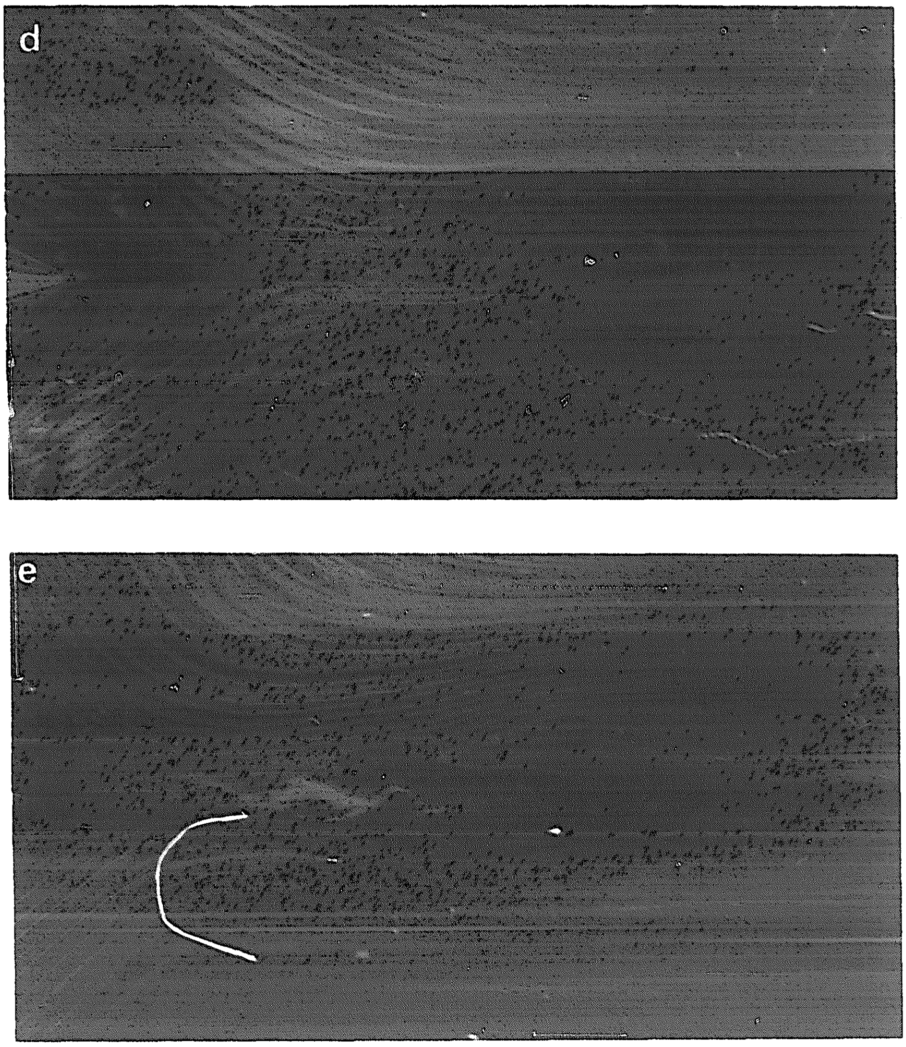

Plate I. Evolution and non-linear saturation of two-dimensional instabilities into large vortical structures in two-dimensional jets. Figures a through e cover Reynolds number ranges from 100 to 10000. (Colors are natural and due to the color interference process.)

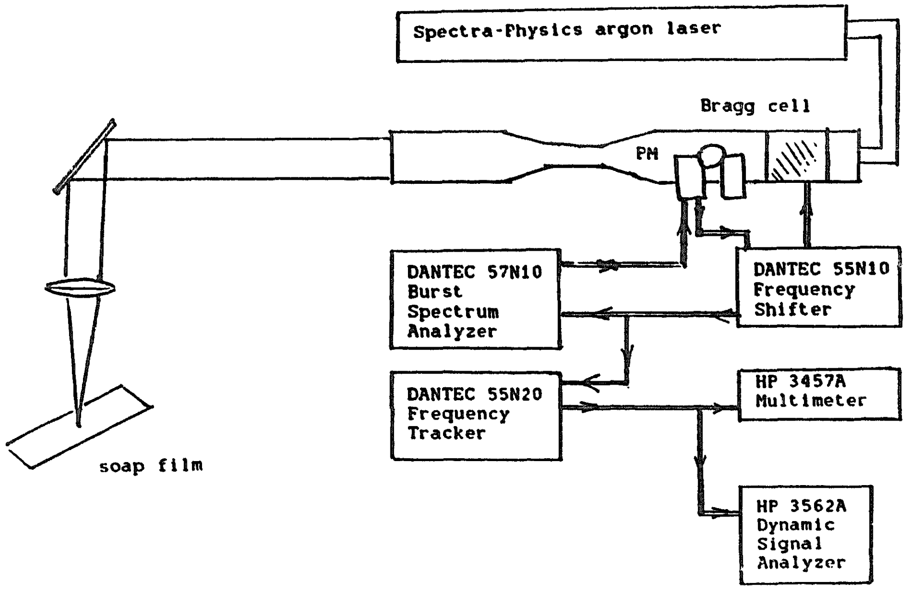

Fig. 8. Schematics of the laser Doppler set-up for velocity measurement in the soap film tunnel.

ber are related by

$$ST = \frac{FD}{V} = 0.212 - \frac{4.5}{Re},$$

where ST is the Strouhal number, F is the shedding frequency, D is the cylinder diameter, V is the free stream velocity and Re is the Reynolds number. Fig. 12 shows Roshko's experimental data and the proposed fitted curve.

We assumed that if there exists a similarity in the dynamics of the two- and three-dimensional cases then Roshko's equation should be able to provide an estimate of μ_F. This was checked by measuring the velocity and frequency of shedding processes of a known size cylinder in the film and then using the Strouhal number to obtain the Reynolds number and consequently the film viscosity from Roshko's equation. The assumption

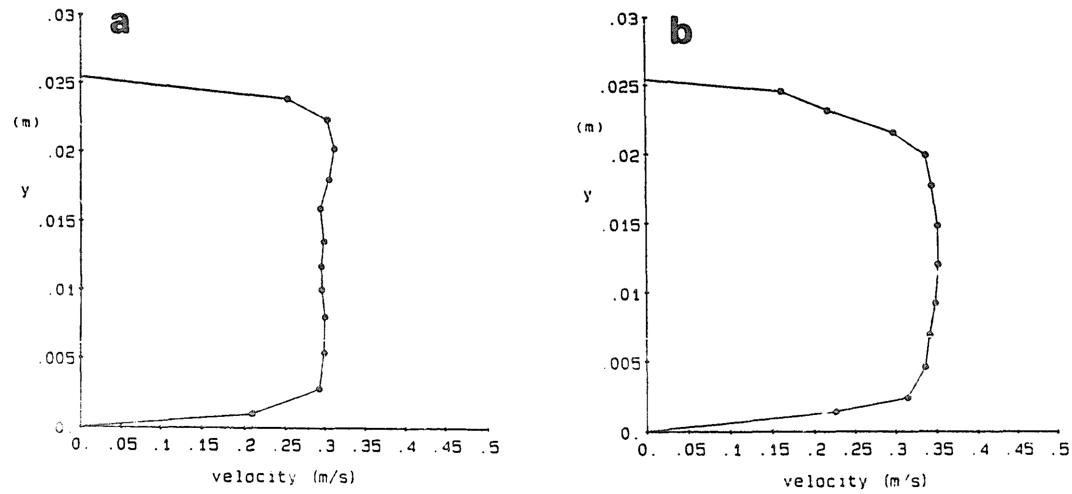

Fig. 9. (a) Mean velocity profile 4 cm from test section entrance. (b) Mean velocity profile at the 10 cm position showing development of boundary layers on the side walls.

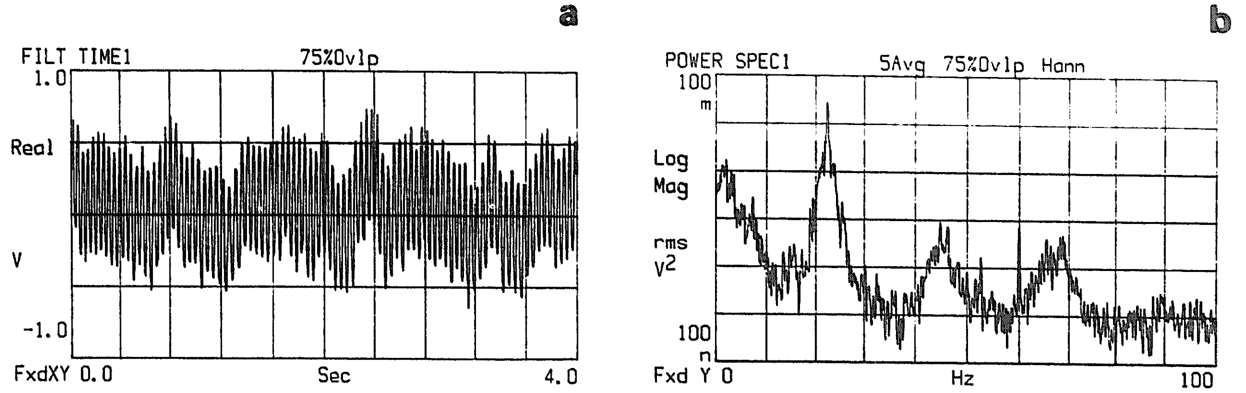

Fig. 10. (a) Time series representing two-dimensional vortex shedding in fig. 4. (b) Power spectrum of the time trace in fig. 10(a). Sharp peak at 22.5 Hz is associated with the vortex shedding frequency.

was that if this viscosity is a true representation of the film viscosity, then by using the empirically determined film viscosity, one should be able to construct Roshko's curve for the two-dimensional vortex shedding process in the soap film tunnel. Fig. 13 represents the construction of one such curve. The viscosity was obtained at the point identified by the arrow. Fig. 13 conveys two main messages. First, the two-dimensional vortex shedding process at a macroscopic level shows a strong similarity to its three-dimensional counterpart. Second, the vortex shedding process can be used as a practical method to estimate film viscosity. It should be noted that we did not extend our data of fig. 13 beyond the transitional Reynolds number (≈ 200) in the cylinder wake flows.

6. Two-dimensional turbulence

Plates I(c) through I(e) display the transition of a jet to a regime that is usually considered to be turbulent. This regime is a unique laboratory example of two-dimensional vortex breakdown in the absence of vortex stretching mechanisms.

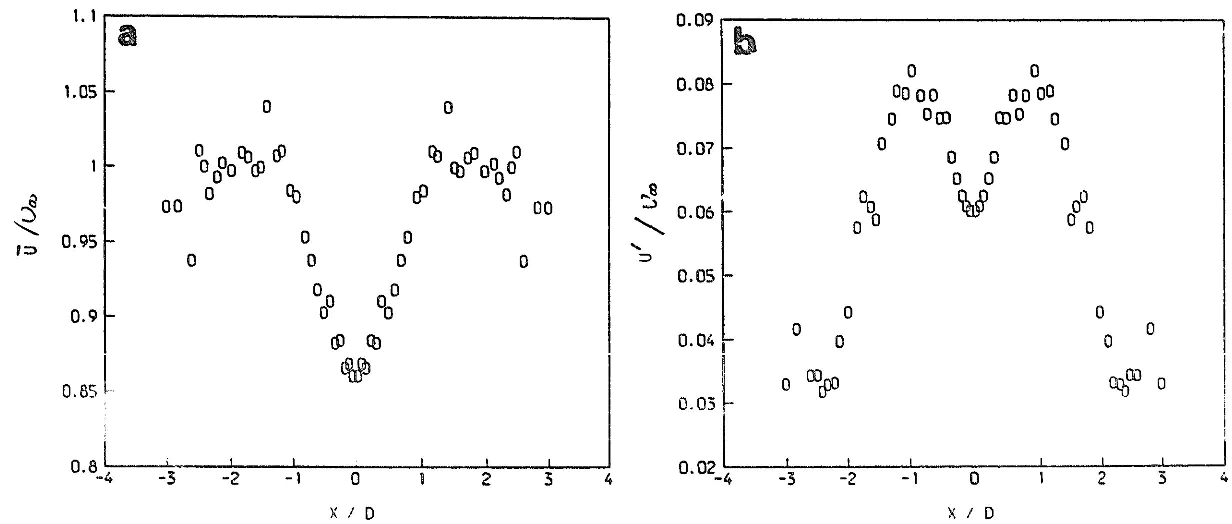

Fig. 11. (a) Mean velocity profile of the wake of the cylinder in fig. 4. (b) RMS velocity fluctuations in the wake of the cylinder in fig. 4.

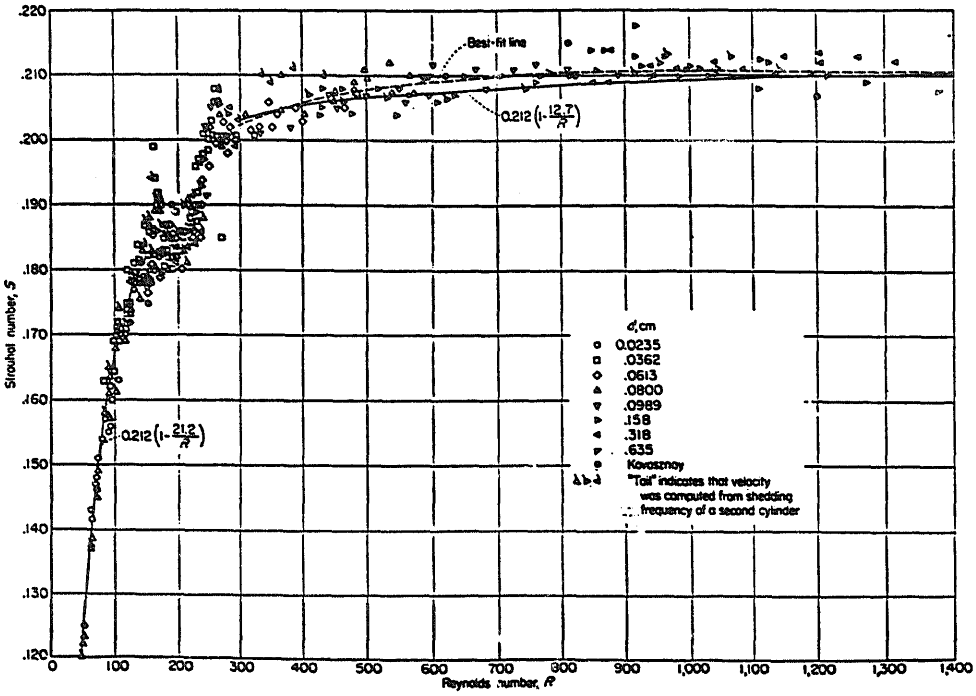

Fig. 12. Strouhal number versus Reynolds number for circular cylinders (from Roshko 1953).

In this preliminary work we attempted to examine the double-cascade concept (Kraichnan [14], Leith [15], Batchelor [16]) for the two-dimensional jet flow as well as for grid-generated turbulence. The heart of the question is whether the energy moves from small scales (injection scale) toward larger scales. It should be mentioned that many recent numerical approaches to this problem suggest that the energy spectrum could significantly deviate from the law given by the phenomenological theory (Babiano et al. [17]).

The velocity fluctuation spectrum (fig. 14) corresponding to the jet in plate I(c) shows a strong sharp peak at the frequency associated with the passage of large vortical structures in the jet. Further downstream (or similarly at higher velocities) in the turbulent region of the jet, the spectrum (fig. 15) contains a broadened region toward lower

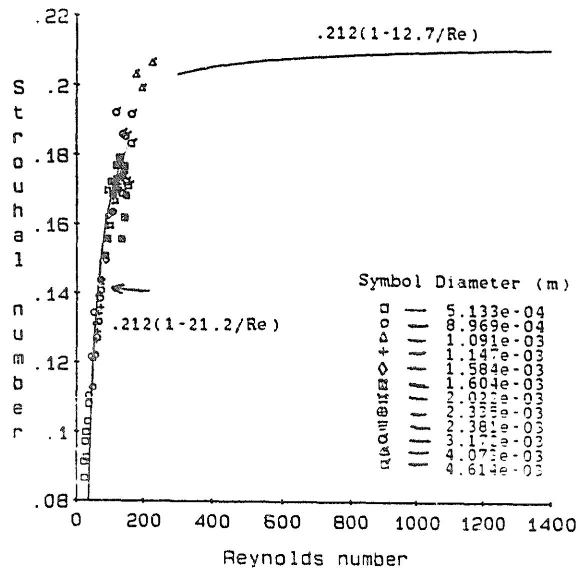

Fig. 13. Strouhal number versus Reynolds number for various circular cylinder wakes in the soap film tunnel.

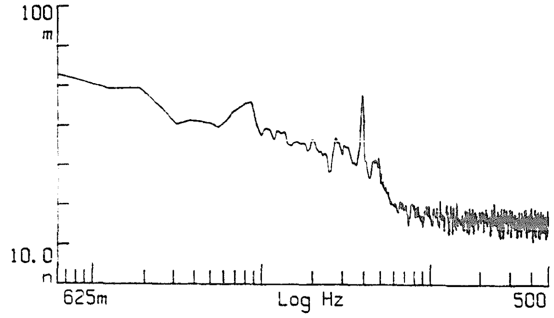

Fig. 14. The velocity fluctuation spectrum corresponding to the initial stages of the jet in plate I(c).

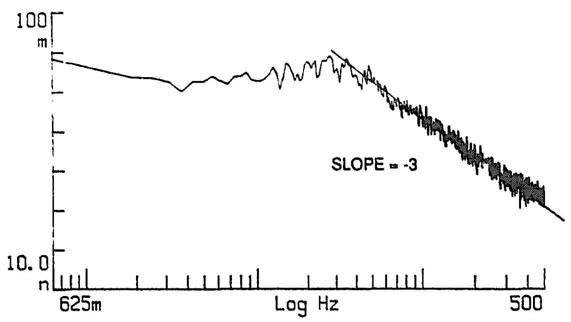

Fig. 15. The velocity fluctuation spectrum corresponding to the turbulent downstream regions of the jet in plate I(c).

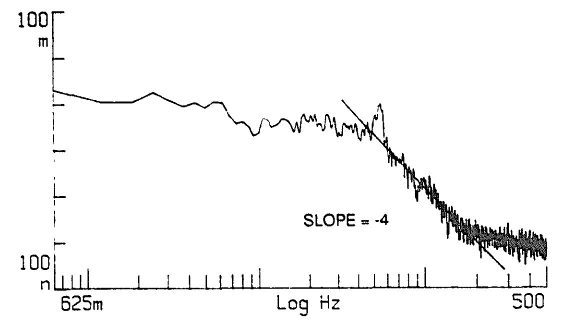

Fig. 16. The velocity fluctuation spectrum corresponding to grid generated flow showing the injection scale, at $x/m = 24$ (where x is downstream distance and m is the grid size).

frequencies and a decay region which is strongly dominated by a k^{-3} cascading process for higher frequencies.

Similar preliminary studies on the grid-generated turbulence suggest that initial injection scale is followed by a k^{-4} cascading region (fig. 16). Spectrum of the velocity fluctuations at a further downstream station (fig. 17) suggest that the peak at the injection scale marks the intersection between two regions of cascading with different slopes. The lower region suggests a $k^{-5/3}$ cascading while the higher frequency region suggests a k^{-3} slope.

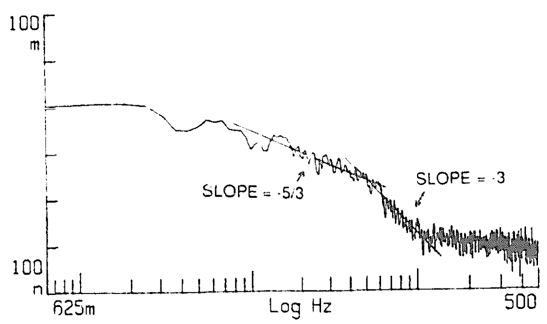

Fig. 17. The velocity fluctuation spectrum corresponding to grid generated flow, at $x/m = 43$.

7. Concluding remarks

Even in this preliminary stage, the soap film tunnel promises a great potential for understanding basic two-dimensional flow phenomena. Future work with this novel device is designed to address current crucial issues of fluid mechanics including turbulence production near the wall in boundary layers, understanding of mixing processes in shear flows, and two-dimensional vortex dynamics and turbulence which for years have lived only as models and theories.

Acknowledgements

We are grateful to Dr. K.J. Mysels for his support and many stimulating discussions. We would also like to acknowledge the valuable assistance of Dr. K. Stuber in the application of laser Doppler velocimetry techniques to soap film flows. This work is currently supported by a grant from the National Science Foundation.

References

[1] R.H. Kraichnan and D. Montgomery, Rep. Prog. Phys. 43 (1980) 547.
[2] D. Lilly, in: Dynamic Meteorology, P. Morel, ed. (Reidel, Dordrecht, 1973).
[3] P.B. Rhines, Ann. Rev. Fluid Mech. 11 (1979) 401.
[4] J. Jimenez, P. Moin, R. Moser and L. Keefe, Phys. Fluids 31 (1988) 1311.
[5] H. Aref, Ann. Rev. Fluid. Mech. 15 (1983) 345.
[6] E.J. Hopfinger, F.K. Browand and Y. Gange, J. Fluid Mech. 125 (1982) 505–534.
[7] J. Sommeria and R. Moreau, J. Fluid Mech. 118 (1982) 507.
[8] K.J. Mysels, K. Shinoda and S. Frankel, Soap Films: Studies of Their Thinning and a Bibliography (Pergamon, Oxford, 1959).

[9] Y. Couder and C. Basdevant, J. Fluid Mech. 173 (1986) 225.
[10] M. Gharib and P. Derango, Bull. Am. Phys. Soc. 32 (1987) 2031.
[11] A.A. Trapeznikov, Proc. second Int. Cong. on Surface Activity (1957), 242.
[12] Y. Couder, J.M. Chomaz and M. Rabaud, these Proceedings, Physica D 37 (1989). 384)
[13] A. Roshko, NACA TN 2913 (1953).
[14] R.H. Kraichnan, Phys. Fluids 10 (1967) 1417.
[15] C.E. Leith, Phys. Fluids 10 (1968) 1409.
[16] G. Batchelor, Phys. Fluids Suppl. II, 12 (1969) 233.
[17] A. Babiano, C. Basdevant, B. Legras and R. Sadourn, C.R. Acad. Sci. Paris. 229 (1985) 601.